Chapter 5

Elman Neural Network Tuned Energy Management Strategy to Improve Fuel Economy in an HEV

This chapter focuses on optimal energy sharing between the internal combustion engine and the battery-powered electric motor in a HEV. For this purpose the Elman neural network has been proposed. This chapter presents a literature review on the eleman neural network based EMS, energy management logic for ENN, problem formulation and constraints, mathematical interpretation of ENN based controller, weight assigning process in ENN, structure of ENN, simulation and hardwarte result analysis and summary.

The input parameters to ENN based controller are torque demand, battery state of charge, and regenerative braking. The proposed strategy aims to maximise the fuel economy while maintaining the battery health. A power-split HEV along with EMS is designed, modelled and simulated in MATLAB/Simulink first and then the whole system is validated in real-time using controller hardware in the loop testing platform (CHIL). The FPGA based MicroLabBox CHIL has been employed to test the system behaviour in real-time. The proposed EMS have been compared with conventional strategies and the comparison reveals that the Elman neural network-based method results in higher fuel economy, faster response, and minimal mismatch between desired and attained vehicle speeds.

5.1 Introduction

The HEVs are comprehended by two energy sources, i.e., internal combustion engine (ICE) and electric motor (EM) which can work together or separately. These vehicles are characterized by low gasoline consumption, low toxic emissions and low-cost mode of transportation. The development of efficient miniature size motors, converters and controllers are key to boost the HEVs advancement. A good controller ensures that the energy demand of the vehicle is met with minimal consumption of gasoline without deteriorating the vehicle performance. Therefore, intelligent and fast controllers are required to achieve optimal energy sharing between the available energy sources in an HEV.

ENN, is predictive in nature, offers higher structural complexity and global optima and has not been explored extensively in the HEV applications. Here, an attempt is made to check the vehicle performance with these two contrary approaches. The ENN used here to ensure that both the sources (ICE and EM) operate in their efficient region with optimal power split. The below section provides a brief review of ENN-based energy management strategies (EMS) for HEVs.

5.1.1 Elman neural network-based energy management strategy

The ANN can be categorised into three different forms i.e. Back propagation neural network (BPNN), Radial basis function neural network (RBFNN) and Elman neural network (ENN). BPNN is associated with the problems like a) slow training rate b) trapping in local minima, c) complex structure for large size network and, d) usage of hit and trial method for choosing the neurons in a hidden layer. RBFNN is used to overcome the slow learning rate and has comparatively less chances to trap in local minima. For further improvement in forecasting accuracy, ENN is applied due to its virtue of dynamic adaptability. It comprises of 4 layers viz. input, hidden, context and output layers. Context layer works as a short-term memory layer and provides previous state output of the hidden layer. The weights of the context layer are kept unity. Thus, this kind of network is adaptable to deal with the dynamic behaviour of a system. The ENN controller is made of the enormous number of interconnected parallel processed elements and offers a quick response with no extra time-delay as in case of BPNN and RBFNN which makes it a perfect choice for responding to driver demand.

In [279], [280] an ANN-based trip model was developed for a highway to improve model accuracy and the fuel economy of the vehicle. In [185], deep learning techniques have been used to identify the driver-specific vehicle speed profile over a repeated drive cycle, which has been used to minimize the amount of fossil fuel. In [281], ANN-based EMS was used for an HEV considering the speed of the vehicle, power at the wheels, and the SoC of UC as inputs to ANN.

A deep reinforcement learning framework for HEV power management aiming to improve fuel economy has been presented in [282]. The energy optimization of plug-in hybrid electric vehicles (PHEV) based on ANN for an unknown trip has been discussed in [283]. In [284], ANN-based optimization has been used with parameters like FC power, SoC, and forecasted power demand with output as the FC power. The modelling and control of the HEV traction system are presented in [285], [286] using NN. In [186], [287], ANN-based EMS was applied to a PHEV having three accessible inputs, current demanded power, ratio of the distance travelled to the total distance and SoC. Here, Pontryagin's minimum principle has also been used to get prior knowledge in terms of data sets. In [288], ANN-based EMS was applied to an HEV having inputs as load current, load power, energy and velocity. In [289], ENN based optimization was carried out on a parallel-HEV with input parameters as torque, speed and SoC. The main contribution of the presented work was to reduce the control reaction time greatly and overcomes the disadvantage of the poor real-time performance of the instantaneous optimal control strategy.

5.2 Power-split HEV configuration and components specification

The Power-split HEV configuration have been employed in this work. The block diagram of this configuration has been shown in Fig. 5.1.

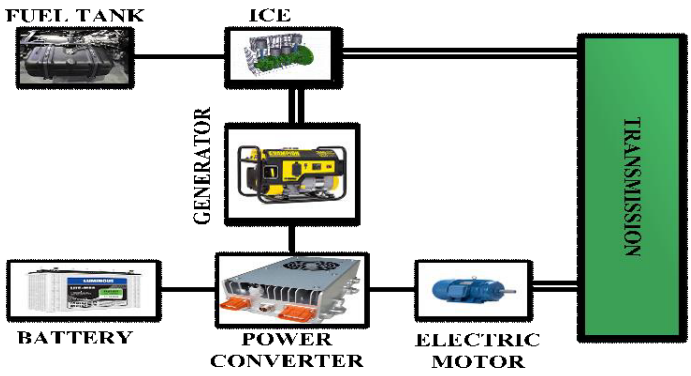

Fig. 5.1. Power-split hybrid electric vehicle

The ON/OFF of the ICE/EM is subjected to the efficient region of their operation, which can be derived from the power versus speed graph given in Fig 4.3 (c) of chapter 4. The motor should be utilized at the beginning (section1-low speed). During this region, the vehicle is in gear position either 1 or 2 and its effectiveness is very high during this tenure. ICE ought to be utilized in section 2. There are some conditions where simultaneous use of EM and ICE is beneficial as shown in section 3. The vehicle and other component specification have been provided in the previous chapter.

5.3 Elman neural network-based EMS for HEV

Energy management logic, boundary constraints and the adopted technique play a critical role in achieving an optimal power split between the available energy sources and are explained below.

5.3.1. Energy management logic

The objective of any EMS is to regulate the flow of energy in a way that the expected speed of the HEV can be achieved. The block diagram of the proposed system is shown in Fig. 5.2. A proportional-integral (PI) block behaves as the driver and generates the requirement of acceleration, braking and driving torque which is fed to the controller. The controller then takes the SoC available from the battery, torques available with the ICE, EM, and generator along with their efficient operating region (Fig. 4.3) and certain other constraints as mentioned in section 5.3.2 below. The controller processes this information as per the EMS, and outputs the torque to be supplied from ICE, EM and generator and the position of ICE throttle. Therefore, the designed EMS decides the ICE, EM, and generator ON/OFF conditions to fulfil the driving torque requirement. This would also ensure that ICE, EM, and generator operate in their efficient region and smooth operation of the vehicle is achieved.

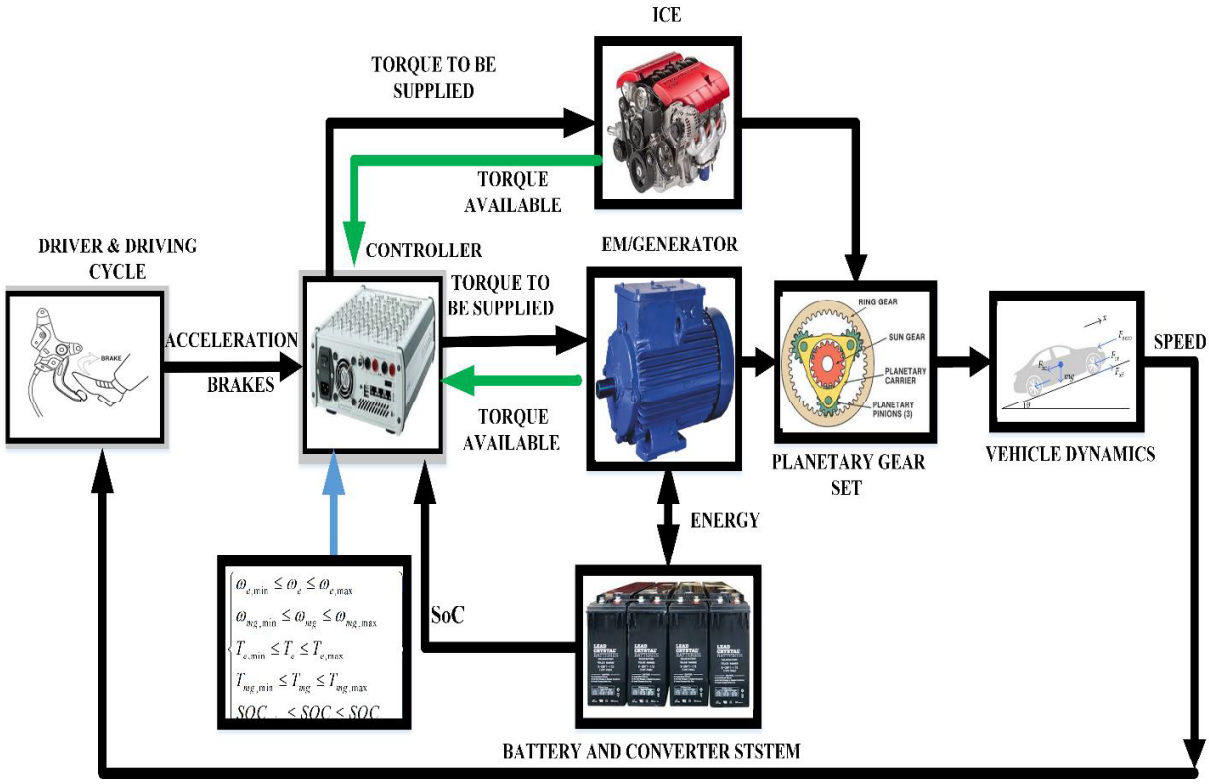

Fig. 5.2. Block diagram of the setup

5.3.2. Problem formulation and Constraints

The problem is formulated to reduce fuel consumption.

$$J = \dot{m}_{ft} \tag{5.1}$$

$\dot{m}_{ft}$ is the total fuel consumption in a driving cycle. $\dot{m}_{ft}$ is the time rate of fuel consumption and is written as

$$\dot{m}_{ft} = \frac{P_{engine} \times g_e}{1000 \times \gamma_f}(l/h) \tag{5.2}$$

P_{engine} is the engine power, g_e is the specific fuel consumption, γ_f is the mass density of fuel (kg/l).

The total consumption in the driving cycle is given by

$$m_{ft}^{\bullet} = \frac{P_{engine} \times g_e}{1000 \times \gamma_f} \Delta t_i \tag{5.3}$$

$$\left.\begin{aligned} P_{bat} &= OCV \times I_{bat} - I^2{}_{bat} \times R_{bat} \\ SoC^{\bullet} &= -\frac{I_{bat}}{Q_{bat}} \end{aligned}\right\} \tag{5.4}$$

Fuel consumption is inversely proportional to the battery power P_{bat}. A greater battery power will cause the vehicle to consume lesser fuel and vice-versa. P_{bat} is directly proportional to battery SoC as given below:

Where $SoC^{\bullet}$ is the rate of change of SoC, OCV is open-circuit voltage, P_b is the battery power, R is the resistance offered by the battery cell, Q_{bat} is the battery capacity.

Where *OCV* is open-circuit voltage, $SoC^{\bullet}$ is the rate of change of SoC, Q_{bat} is the battery capacity, I_{bat} is the battery current and R_{bat} is the internal resistance of the battery.

The relation between *mg1*, *mg2*, *ICE*, and requested torques T_{mg1}, T_{mg2}, T_e, T_{req} and speeds ω_{mg1}, ω_{mg2}, ω_e, ω_{req} can be understood from the following equations.

$$T_{mg1} = -\frac{1}{1+R}\left[T_e\right] \tag{5.5}$$

$$\omega_{mg1} = -R \times \zeta \times \omega_r + \left(1+R\right) \times \omega_e \tag{5.6}$$

$$T'_{mg2} = -\frac{1}{\left(1+R\right)}\left[-\frac{\left(1+R\right) \times T'_{req}}{\zeta} + R \times T'_e\right] \tag{5.7}$$

$$\omega_{mg2} = \zeta \times \omega_{req} \tag{5.8}$$

In the above equations, R and ζ represent the gear ratio of Planetary gear set and the final drive ratio respectively.

$$\left.\begin{aligned} P_{bat} &= T_{mg1}\omega_{mg1}\eta_{mg1}^{k_{mg1}} + T_{mg2}\omega_{mg2}\eta_{mg2}^{k_{mg2}} \\ where, k &= \begin{Bmatrix} +1, T_i\omega_i > 0 \\ -1, T_i\omega_i < 0 \end{Bmatrix}, i = \{mg1, mg2\} \end{aligned}\right\} \tag{5.9}$$

For any smart control design, it is necessary to satisfy the constraints given in equation (5.10) below.

$$\left\{\begin{aligned} &\omega_{mg,\min} \le \omega_{mg} \le \omega_{mg,\max} \\ &T_{e,\min} \le T_e \le T_{e,\max} \\ &T_{mg,\min} \le T_{mg} \le T_{mg,\max} \\ &SoC_{\min} \le SoC \le SoC_{\max} \end{aligned}\right\} \tag{5.10}$$

Where, $\omega_{e,\min}$, $\omega_{e,\max}$, $\omega_{mg,\min}$, $\omega_{mg,\max}$, $T_{e,\min}$, $T_{e,\max}$, $T_{mg,\max}$, $T_{mg,\min}$, $SoC_{\min}$ and $SoC_{\max}$ are the minimum and maximum values of speed and torque of the engine, motor and generator set, and SoC respectively. FLC and ENN-based algorithms are developed considering the constraints to achieve the power demand of HEV.

5.3.3 Mathematical interpretation of ENN based controller.

The inputs to ENN are the torque demand, brakes, and SoC value of battery and outputs are EM, generator and ICE torque respectively. The number of hidden neurons is to be selected on the basis of least Mean Square Error (MSE) as in Table 5.1. The ENN mainly consists of the input layer, hidden layer, context (undertaken) layer, and output layer.

The input vector is a three dimensional denoted by vector u and output layer is also a three-dimensional vector and is denoted by y. The output vector of the hidden layer is n-dimensional vector x. The output vector of the context layer is n-dimensional vector r. The connective weights (w) of the hidden layer are w_1, w_2 and w_3, $g(\square)$ is the driving function of the output neurons, $f(\square)$ is the driving function of the hidden layer, $net(\square)$ is the net input driving function of a certain layer;

A represents the input layer; B represents the context layer and *K* shows the iterative sequence. A brief mathematical modelling of ENN is given below:

If, functions

$$v_i(k)=\begin{Bmatrix} u_n(k), if\ i \varepsilon A \\ r_n(k), if\ i \varepsilon B \end{Bmatrix} \tag{5.11}$$

$$w_i(k)=\begin{Bmatrix} w^2, if\ i \varepsilon A \\ w^3, if\ i \varepsilon B \end{Bmatrix} \tag{5.12}$$

Then input and output functions of the hidden layer are

$$\left.\begin{aligned} net_n(k+1) &= \sum_{i \varepsilon A \cup B} w^i(k) v_i(k), \\ x_n(n+1) &= f\left(net_n(k+1)\right) \end{aligned}\right\} \tag{5.13}$$

Input and output functions of undertaken layer are

$$\left.\begin{aligned} net_n(k) &= \sum_{i \varepsilon A \cup B} w^i(k-1) v_i(k-1), \\ r(k) &= h\left(net_n(k)\right) \end{aligned}\right\} \tag{5.14}$$

and input and output functions of the output layer are

$$\left.\begin{aligned} net_n(k+1) &= \sum_{i \varepsilon A \cup B} w^i(k+1) x_n(k+1), \\ y_n(k+1) &= g_n\left(net(k+1)\right) \end{aligned}\right\} \tag{5.15}$$

5.3.4.1 ENN Parameters can be selected by the following steps.

The number of neurons used in ENN is estimated by

$$k=\sqrt{j+n}+\beta \tag{5.16}$$

where j is the number of the input vector; n is the neuron number of the output vector; β is a constant.

The excitation function of ENN of the feedback layer selects the 'Tansig' function

$$Tansig(x)=\frac{2}{1+e^{-2x}}-1 \tag{5.17}$$

5.3.4.2. Estimation of Learning and Training Mechanism of ENN

ENN is trained by Levenberg- Marquardt algorithm. The error-index function of Levenberg- Marquardt arithmetic is

$$E(w)=\frac{1}{2}\sum_{i=1}^{p}\left[y_i - y_i^{'} \right]=\frac{1}{2}\sum_{i-1}^{p}e_i^2(w), \tag{5.18}$$

where p is the sample number; e^i is the systemic error; $y_i^{'}$ is the actual output of the network.

5.3.4.3. The formula of the adjusting weight is

$$w^{k+1}=w^k+\Delta w \tag{5.19}$$

5.3.4.4. The increment weight is

$$\Delta w=\left[J^T(w)J(w)+uI \right]^{-1}J^T(w)e(w), \tag{5.20}$$

where u is learning rate; I is the unit matrix; $J(w)$ is the Jacobian matrix. Consider

$$J(w)=\begin{bmatrix} \frac{de_1(w)}{dw_1} & \frac{de_1(w)}{dw_2}\cdots\cdots & \frac{de_1(w)}{dw_n} \\ \frac{de_2(w)}{dw_1} & \frac{de_2(w)}{dw_2}\cdots\cdots & \frac{de_2(w)}{dw_n} \\ \frac{de_n(w)}{dw_1} & \frac{de_n(w)}{dw_2}\cdots\cdots & \frac{de_n(w)}{dw_n} \end{bmatrix} \tag{5.21}$$

The Fig. 5.3 demonstrate the weight adjusting process of ENN.

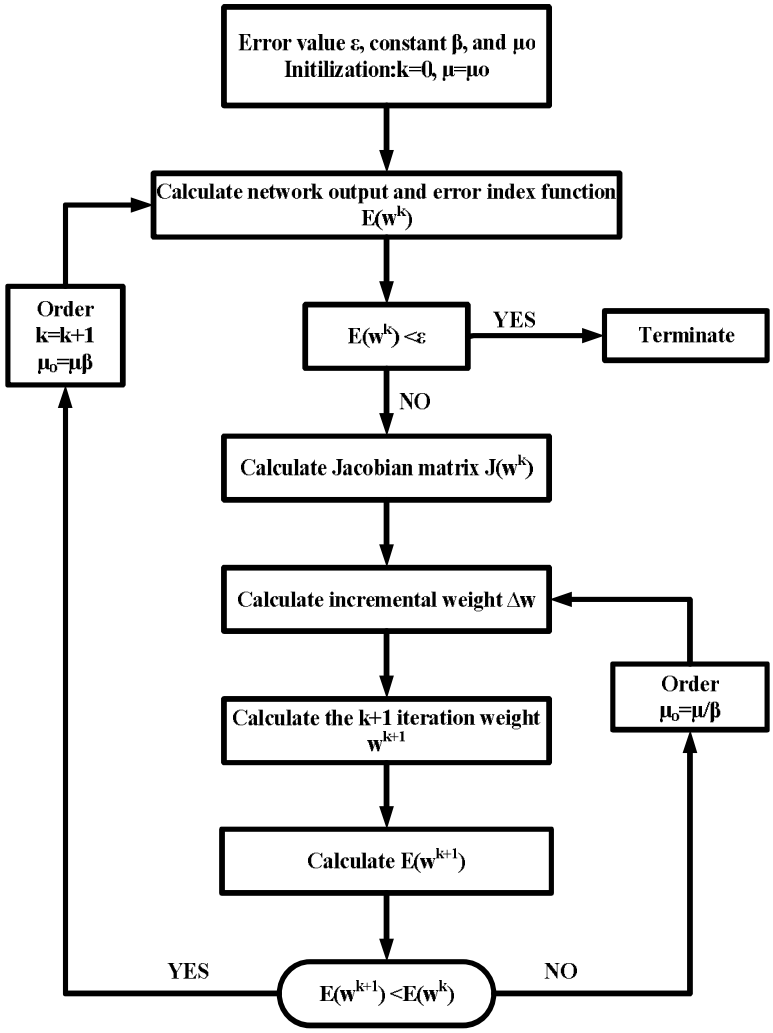

Fig. 5.3. Weight assigning process in ENN

ENN requires prior knowledge in the form of a data set. Here, the input data comprises of SoC, brakes, torque requirement, torque available and efficient region of operation of sources. The output is the torque to be delivered from motor, generator, and ICE. This data is fed to the ENN, which trains this data to obtain the optimal torque/power split among available sources while these operate in their efficient regions. The structure of the NN for the proposed work is shown in Fig. 5.4(a).

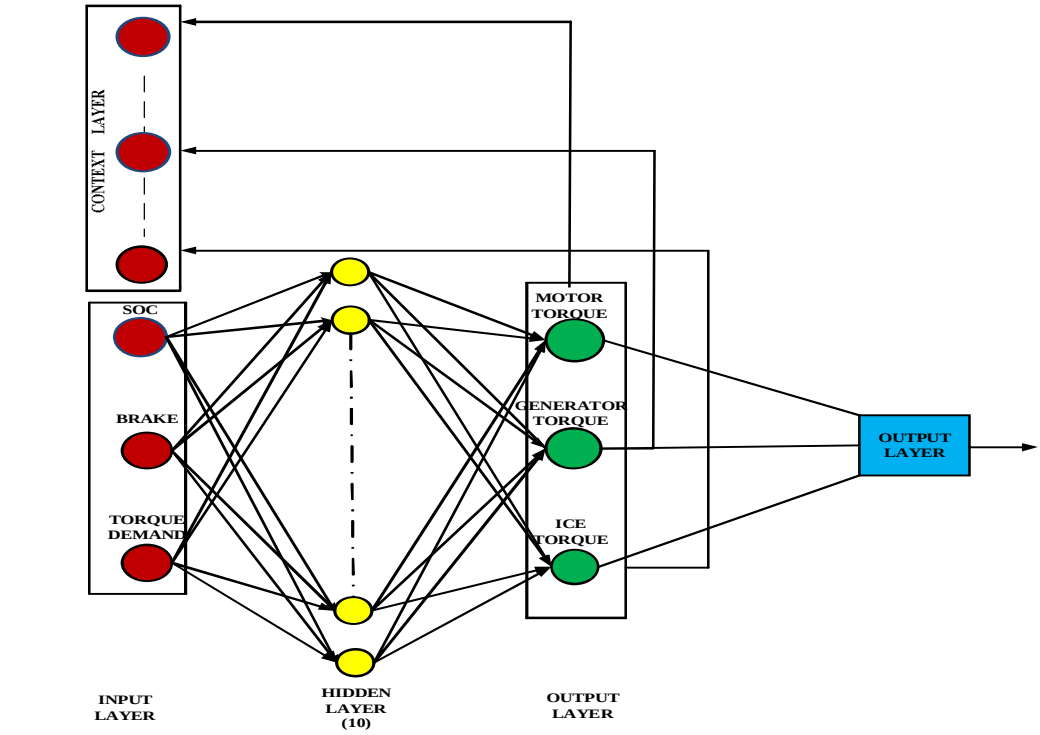

(a) Structure of the ENN

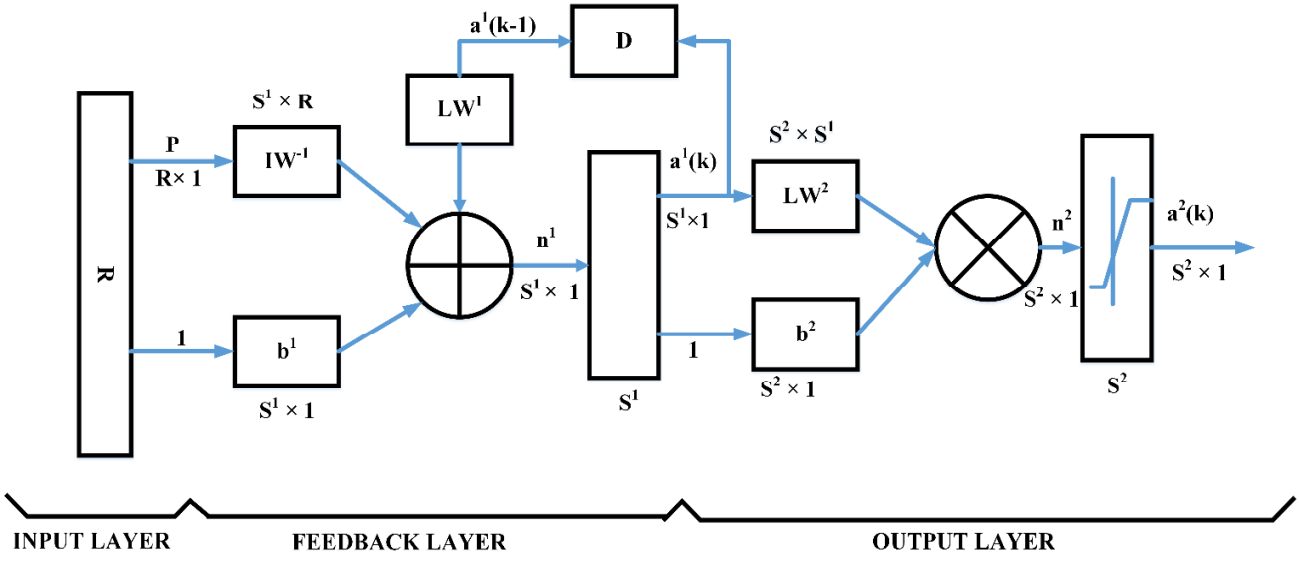

(b) Mathematical model of ENN

Fig. 5.4 Structure of the ENN and the mathematical model of ENN.

Where:

P is the input fed to the ENN having size $R\times 1$.

b^1 is considered as the threshold vector of the feedback layer with size $S^1\times 1$.

IW^1 where W is the connective weight vector, and I is input vector of the input layer with size is D.

n^1 is the middle operational result of the feedback layer, namely, weighted sum of the connective weight vector and the threshold vector, and its size is $S^1 \times 1$.

a^1 is the output vector of the feedback layer's neuron in the k iteration and its size is $S^1 \times 1$.

D is the feedback node. In the similar manner the parameters b^2, LW^2, n^2 and a^2 are related to the output layer.

The specification of the ENN used here are given in Table 5.1.

Table 5.1 The ENN Specifications

Training based on	Levenberg-Marquardt
Performance	Mean-squared error
Iteration	227
Learning ratio	0.1
Number of hidden layer nodes	10

5.4 Simulations and Hardware Results

The simulation has been carried out in Simulink/MATLAB. The whole system is validated in real-time on CHIL testing platform using FPGA based MicroLabBox. The CHIL laboratory setup for the validation of the simulated results is shown in Fig. 5.5. The result obtained through simulation and real-time CHIL are provided with the explanatory inference below in Fig. 5.6 and Fig. 5.7.

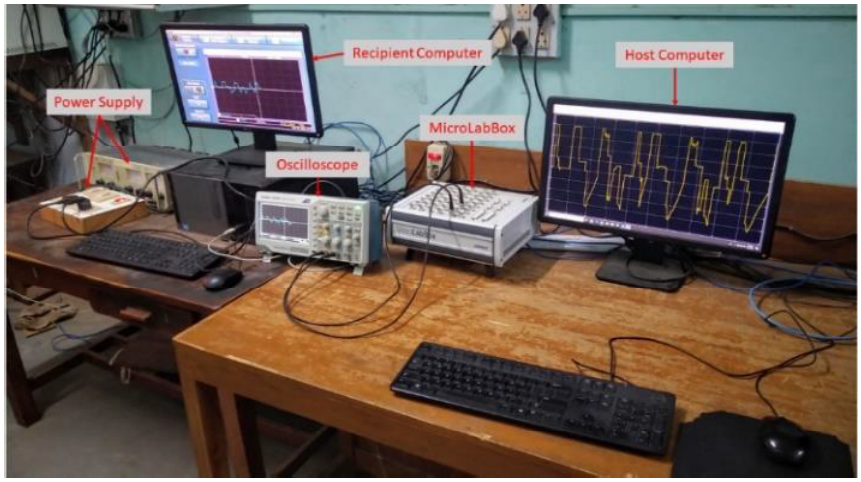

Fig. 5.5. CHIL Setup of the System

****In Fig. 5.6 and Fig. 5.7, S and H represent the simulation and the CHIL results respectively. The real-time results are in close resemblance to simulation results. All abscissa axis is for t=500s. The result shown is only for 500s as the sampling time of the DSO is 50s, so at a time in one screen it can display the result for 500s.**

The proposed method is tested on many driving cycles, but the results and analysis presented here is for New European driving cycle (NEDC).

Figs. 5.6 (S1) and (H1) demonstrate the SoC variation with various control strategies. It is observed that ENN effectively regulates the charging/discharging of the battery maintaining higher SoC as compared to other techniques. The fuel consumption is measured in Mileage (Km/L) and Miles per gallon (mpg) in simulation results. As shown in Fig. 5.6 (S2) and Fig. 5.6 (S3) and Fig. 5.6 (H2) and Fig. 5.6 (H3) the ENN-based approach provides higher fuel economy over the same driving cycle as compared to FLC based and conventional approaches. The CHIL results also show a close resemblance with simulation results, which holds the accuracy and integrity of the work done.

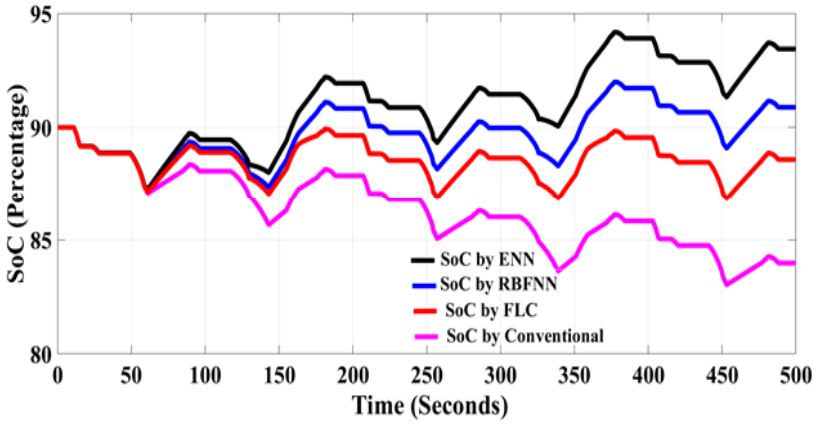

(S1) SoC with ENN, RBFNN, FLC, and Conventional Strategy

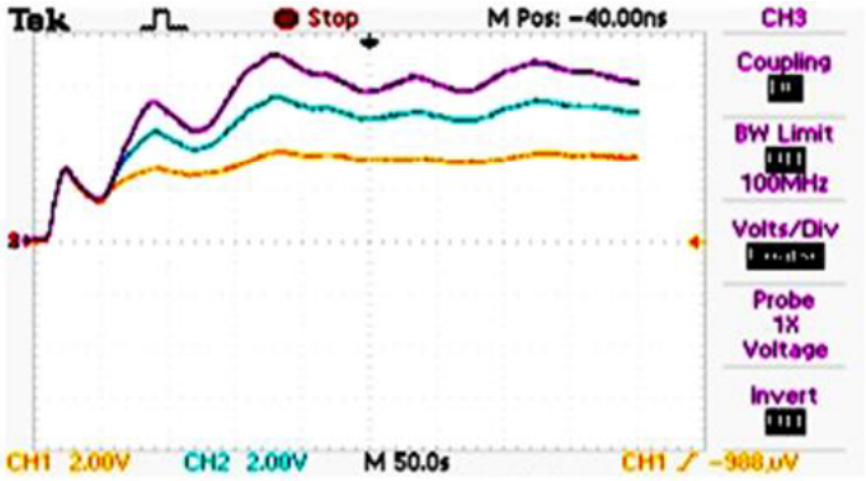

(H1) SoC with ENN, RBFNN, FLC, and Conventional Strategy

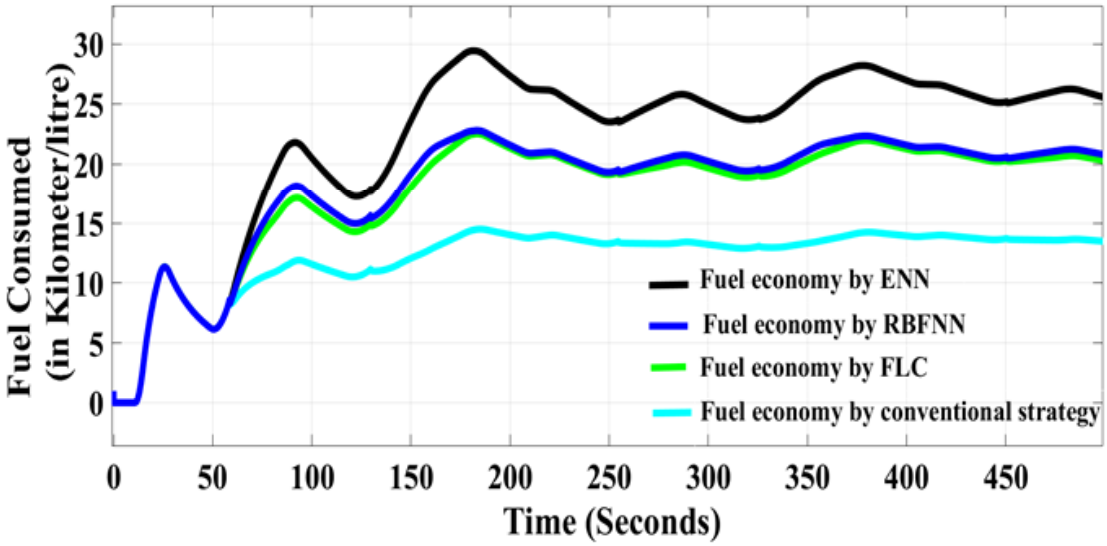

(S2) Fuel economy Kilometer/Litre with ENN, RBFNN, FLC, and Conventional Strategy

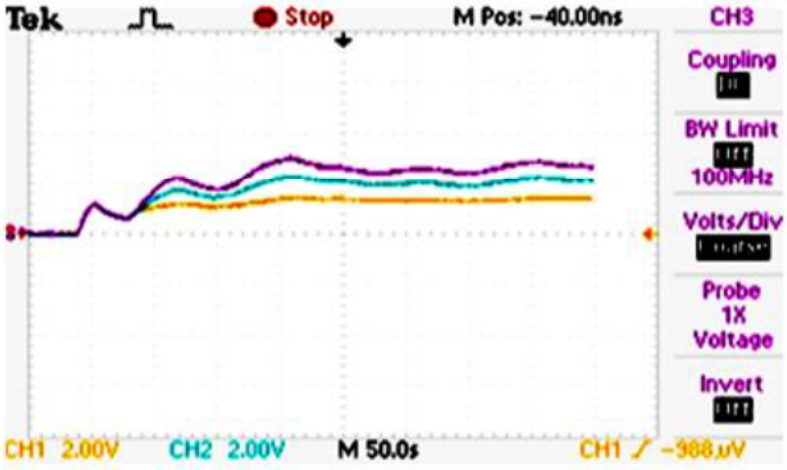

(H2) Fuel economy Kilometre/Litre with ENN, FLC, and Conventional Strategy

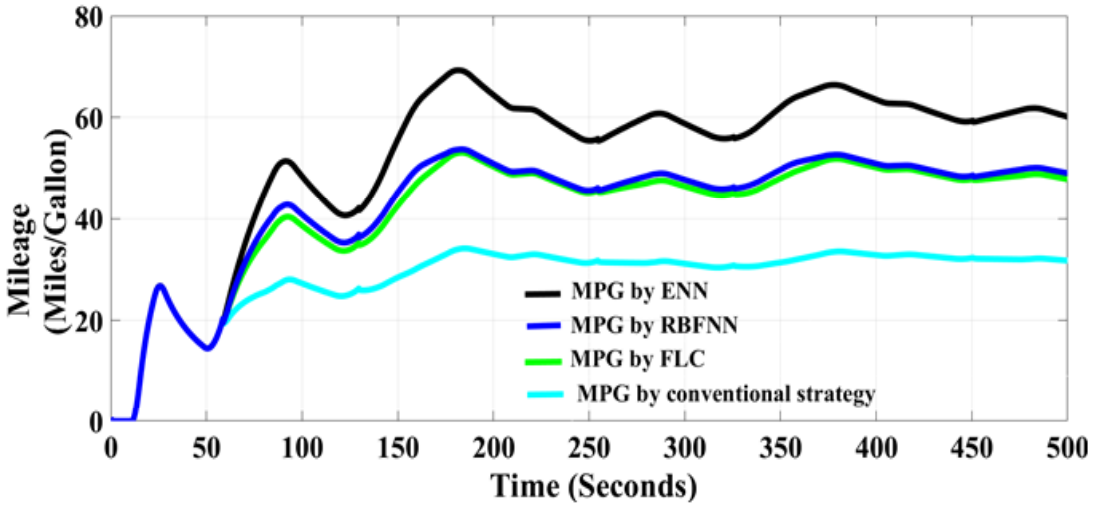

(S3) Miles per Gallon consumed with ENN, RBFNN, FLC, and Conventional Strategy

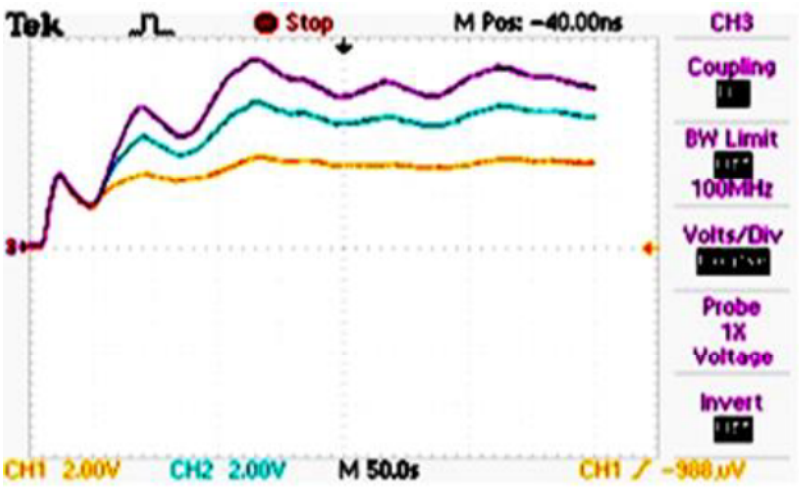

(H3) Miles per Gallon consumed with ENN, FLC, and Conventional Strategy

Fig. 5.6 The comparison of the SoC and fuel economy in (Km/L and Miles per Gallon).

Vehicle speed must encounter the expectation of the driving cycle. If the achieved vehicle speed matches with the driving cycle, leaving no trace and completely coinciding, then it is considered an ideal condition. An efficient algorithm always checks that the desired speed is achieved. Fig. 5.7 (S1) depict the achieved and desired speeds by FLC strategy. The red and blue lines don't collide over each other leaving a miss trace. Hence the trace missing can be seen in these speeds. Fig. 5.7 (S2) depicts the desired and achieved speed graphs using the ENN controller. These speed graphs are almost coinciding, i.e., leaving

no trace missing. This proves that the proposed ENN-based method offers better drivability of the vehicle.

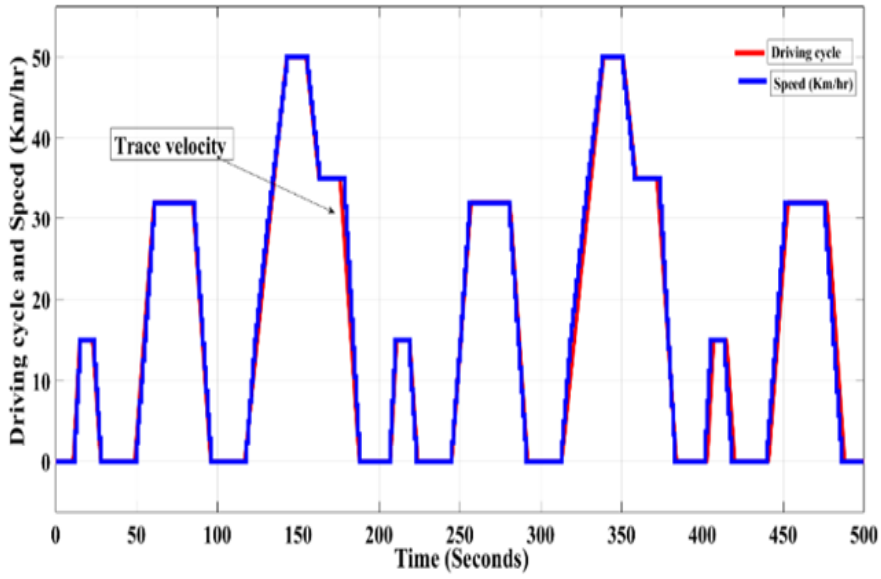

(S1) Desired and achieved speeds of the vehicle using FLC (the red and blue lines don't overlap each other, leaving a miss trace)

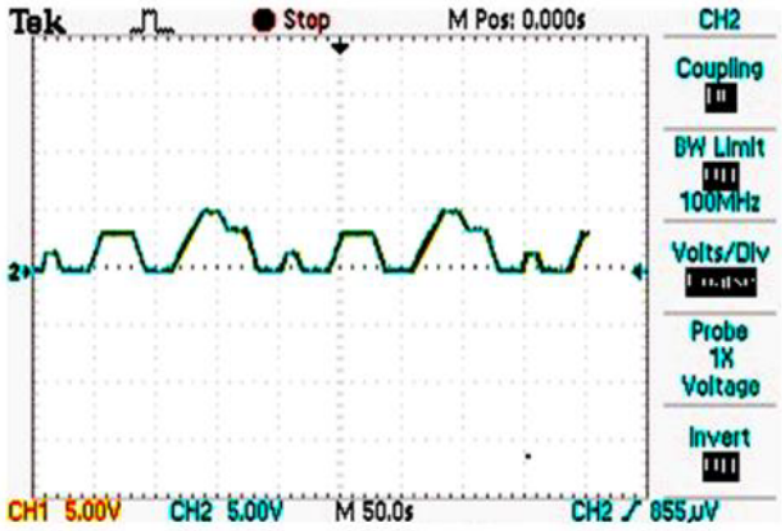

(H1) Desired and achieved speeds of the vehicle using FLC

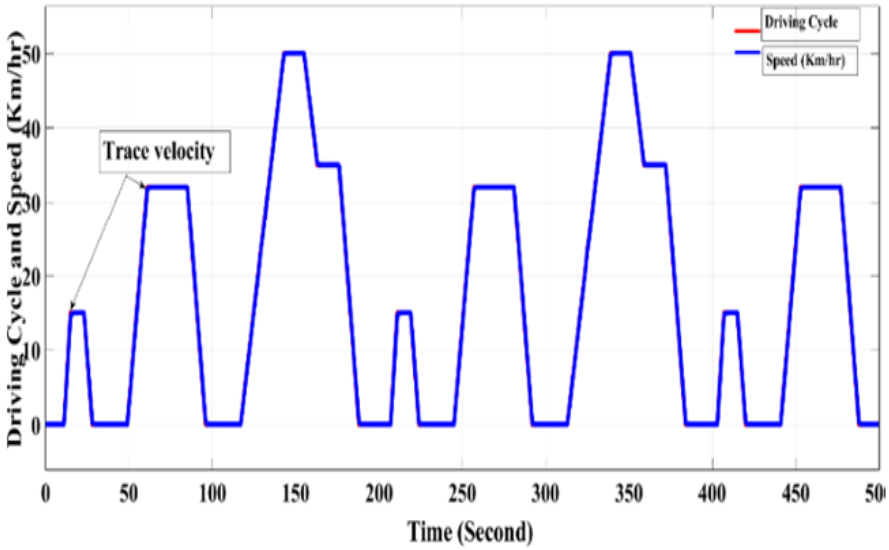

(S2) Desired and achieved speeds of the vehicle using ENN (the red and blue lines overlap each other, leaving no miss trace)

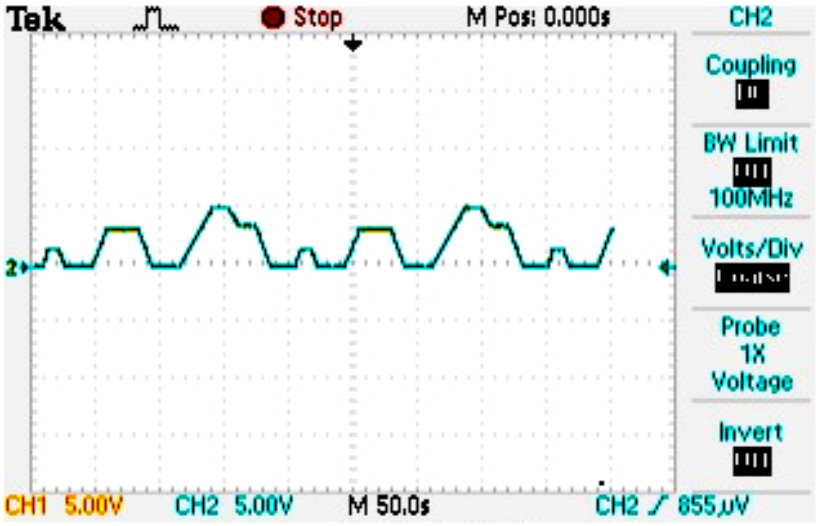

(H2) Desired and achieved speeds of the vehicle using ENN

Fig. 5.7 The comparison speed trace miss between FLC and ENN

A comparison of the fuel economy obtained using the proposed methods and the methods available in the literature is shown in Table 5.2. The fuel economy obtained using proposed ENN and FLC is far better than the conventional controllers. Also, the proposed ENN-based strategy yields the highest fuel economy over other similar methods.

Table 5.2 Comparison of fuel economy and optimisation methods for power-split HEV

EMS used in the proposed work	Claimed outcomes
Conventional strategy	The fuel consumption is NEDC - 13.49 Km/L and 31.72 mpg UDDS - 20.5 Km/L and 48.4 mpg FTP - 61.13 Km/L and 143.7 mpg
FLC	The fuel consumption is NEDC - 20.31Km/L and 47.77 mpg UDDS - 23.2 Km/L and 54.61 mpg FTP - 63.33 Km/L and 148.9 mpg
RBFNN	The fuel consumption is NEDC- 20.81Km/L and 48.95 mpg UDDS – 24.8 Km/L and 58.73 mpg FTP - 65.53 Km/L and 154.1 mpg
ENN	The fuel consumption for NEDC- 25.56 Km/L and 60.11 mpg. UDDS- 25.5 Km/L and 60.17 mpg. FTP - 69.88 Km/L and 164.3 mpg

5.5 Summary

This investigation presents the design, modelling, and real-time validation of ENN based energy management strategies in HEV. The simulations have been carried out in Simulink/MATLAB environment first and their validation in real-time has been carried out on a controller-hardware-in-the-loop testing setup. The FPGA based MicroLabBox hardware controller has been used to execute the real-time instructions. The strategies are fed with the primary input parameters like driving torque demand, battery SoC, regenerative braking, and several other constraints, including the efficient region of operation for sources. The inputs and constraints fed to EMS, decide the optimal energy sharing among electric motor, IC engine and generator and accordingly decide their turning ON/OFF on board. These strategies regulate the torque in such a way that the engine and electric motor operate in their efficient operating regions. The comparison of the EMS yields that the ENN based strategy offers better fuel economy and faster response with minimal mismatch and achieves the desired speed. There was an improvement of fuel economy in NEDC- from 31.72 mpg to 60.11 mpg, UDDS- 48.4 mpg to 60.17 mpg and for FTP from 143.7 mpg to 164.3 mpg.